Comparative transcriptomic analysis of articular cartilage of post-traumatic osteoarthritis mouse models

Sophie J. Gilbert[1,*], Jamie Soul[2,*,§], Yao Hao[2], Hua Lin[2], Katarzyna A. Piróg[2], Jonathan Coxhead[2], Krutik Patel[2], Matt J. Barter[2], David A. Young[2,‡], Emma J. Blain[1,‡]

[1]Biomechanics and Bioengineering Research Centre Versus Arthritis, Biomedicine Division, School of Biosciences, The Sir Martin Evans Building, Cardiff University, Cardiff, CF10 3AX, Wales, UK
[2]Biosciences Institute, Newcastle University, Centre for Life, Central Parkway, Newcastle upon Tyne, NE1 3BZ, UK

[*]Contributed equally to the study
[‡]Authors for correspondence: david.young@newcastle.ac.uk; blain@cardiff.ac.uk
[§]Present address: Institute of Systems, Molecular and Integrative Biology, University of Liverpool, Liverpool L69 7ZB, UK

Abstract

Animal models of post-traumatic osteoarthritis (PTOA) recapitulate the pathological changes observed in human PTOA. Here, skeletally mature C57Bl6 mice were subjected to either the rapid-onset, non-surgical, mechanical anterior cruciate ligament (ACL) rupture or surgical destabilisation of the medial meniscus (DMM) models. Transcriptome profiling of micro-dissected cartilage at day 7 and 42 post-ACL and DMM procedure respectively, showed that the two models were comparable and highly correlative (Spearman R =0.82, p<2.2E-16). Gene ontology enrichment analysis identified similarly enriched pathways, which were overrepresented by anabolic terms. To address the transcriptome changes more completely in the ACL model we also performed small RNA-seq, describing the first microRNA profile of this model. miR-199-5p was amongst the most abundant yet differentially expressed microRNAs and its inhibition in primary human chondrocytes led to a comparable transcriptome response to that observed in both human 'OA damaged vs intact cartilage' and murine DMM cartilage datasets. *CELSR1*, *GIT1*, *ECE1* and *SOS2* were all experimentally verified as novel miR-199-5p targets. Together, these data support the use of the ACL rupture model as a non-invasive companion to DMM.

Keywords: PTOA, ACL rupture, DMM, microRNA, cartilage

Introduction

Post-traumatic osteoarthritis (PTOA), commonly referred to as secondary OA, accounts for 12% of all patients presenting with OA (Brown et al., 2006) and arises following a known mechanical insult or traumatic injury. Traumatic destabilizing injury to the knee joint in young adults significantly increases the risk of developing OA in middle age (Gelber et al., 2000; Muthuri et al., 2011; Snoeker et al., 2020), particularly following a meniscal tear, intra-articular fracture and after cruciate ligament injury. Approximately 50% of patients with a diagnosed anterior cruciate ligament (ACL) or meniscus tear will develop pain and functional impairment of the joint 10 – 20 years post-injury (Lohmander et al., 2007; Neuman et al., 2008). Epidemiological studies estimate an incidence of 77 in 10,000 patients reporting an acute knee trauma (Peat et al., 2014) and 8 in 10,000 with ACL tears per annum (Sanders et al., 2016). These numbers will likely continue to increase due to a more active demographic which is further compounded by the current lack of diagnosis following a traumatic injury and/or prognostic biomarkers to reliably predict whether OA will subsequently develop (Garriga et al., 2021). Therefore, understanding the aetiology of PTOA is imperative to define the early initiating events and identify effective diagnostics for subsequent treatment.

Several mechanically induced OA animal models have been established to recapitulate the pathological changes observed in human PTOA after an injury. The animal is subjected to a defined traumatic injury and temporal disease progression monitored to characterise the molecular, structural, and functional outcomes. Traumatic injury to destabilise the joint is achieved either following surgical transection or via application of a non-invasive mechanical load (comprehensively reviewed in (Blaker et al., 2017; Christiansen et al., 2015; Narez et al., 2020)); the most commonly used PTOA models include destabilisation of the medial meniscus (DMM) (Glasson et al., 2007) and non-surgical mechanically induced rupture of the ACL (Christiansen et al., 2015; Gilbert et al., 2018). Importantly, both models induce early inflammation, cartilage matrix loss resulting in fibrillation and destruction, synovitis, subchondral bone remodelling and formation of osteophytes (Burleigh et al., 2012; Gilbert et al., 2018; Lieberthal et al., 2015), clinical features which are also observed in human PTOA pathogenesis (Watt et al., 2016).

MicroRNAs (miRNAs) are small non-coding RNAs that regulate gene expression (Bartel, 2009). Studies have previously characterised candidate miRNAs that are regulated in the early phases of OA pathogenesis using the DMM model (Kung et al., 2018; Kung et al., 2017b). Interestingly, transcriptomic analysis did not show an association between miRNA regulation and OA in the synovium (Kung et al., 2017b), subchondral bone (Kung et al., 2018) or serum (Kung et al., 2017a). However, in the articular cartilage a subset of miRNAs was significantly regulated (Kung et al., 2018); functional enrichment and data annotation

revealed responses to mechanical stimulation, apoptotic processes and ECM structural and regulatory factors that are potentially involved in OA pathogenesis. miRNA analyses have also previously been reported in rat surgical ACL transection models with miR-27b (Zhang et al., 2020), miR-122 and miR-451 significantly elevated in the cartilage following joint destabilisation (Scott et al., 2021). To date, there have been no publications characterising the miRNA profile in cartilage harvested from the non-surgical load induced ACL rupture model and only one mRNA transcriptome study reported (Chang et al., 2017). Differential regulation was observed for 1446 genes (including long non-coding RNAs (lncRNAs)) and interestingly, when compared to the mRNA profile of the DMM model, the greatest overlap was observed in the ACL rupture model 1-week post-injury with 4 weeks following DMM (Chang et al., 2017).

Therefore, in this study we aimed to characterise the expression profile of mRNA and miRNAs following mechanically induced ACL rupture to identify miRNAs, and their downstream mRNA targets, that are regulated in the early phases of PTOA disease progression. We also compared the miRNA ACL rupture gene signature with that following DMM and of the miRNAs identified, miR-199a-5p was similarly differentially up-regulated. Inhibition of miR-199a-5p in primary human chondrocytes revealed a role for this miRNA in extracellular matrix organisation.

Materials & Methods

Animals

All animal experiments were performed under licenses [Cardiff: P287E87DF, Newcastle: P8A8B649A] granted from the Home Office (United Kingdom) in accordance with the guidelines and regulations for the care and use of laboratory animals outlined by the Animals (Scientific Procedures) Act 1986 according to Directive 2010/63/EU of the European Parliament and conducted according to protocols approved by the Animal Ethics Committee of Newcastle University or Cardiff University and the Home Office, United Kingdom. Breeding and subsequent phenotyping was performed under licence P8A8B649A. All animal experiments were performed in compliance with the ARRIVE guidelines (Kilkenny et al., 2012). All animals were housed with 12:12 h light/dark photocycles, with food and water available *ad libitum.* A schematic of the experimental design and animals used is provided (Supplementary Figure 1).

Post-traumatic OA models

Destabilisation of the medial meniscus (DMM) model

The destabilisation of the medial meniscus (DMM) surgical model was performed essentially as described previously (Glasson et al., 2007). Briefly, eight C57Bl/6J male mice (25-30 g; bred inhouse from Charles River, UK) at 11-weeks of age were assigned to surgery or non-surgical groups. The surgery group were given a pre-operative analgesic (buprenorphine), anaesthetised (isoflurane) and had their left knee medial meniscus destabilized by transecting the medial meniscus tibial ligament (MMTL) with a needle blade. The surgical wound was closed with Reflex 7mm wound clips which were removed seven days post-surgery. The day after surgery animals were given two doses of buprenorphine subcutaneously ~8 hours apart. Forty-two days post-surgery, mice were euthanised, by cervical dislocation.

Anterior cruciate ligament (ACL) rupture model

Twelve-week-old male C57Bl/6J mice (~25 g; Envigo, Huntington, UK) were randomly assigned to either experimental or control groups and randomly allocated to cages in groups of four or five. The ACL rupture model was performed as described previously (Gilbert et al., 2018). Briefly, mice were anaesthetized with isoflurane and custom-built cups used to hold the right ankle and knee in flexion with a 30^{o} offset prior to the application of a 0.5 N pre-load (ElectroForce3200; TA Instruments, Elstree, UK). A single 12 N load at a velocity of 1.4 mm s^{-1} was then applied resulting in anterior cruciate ligament (ACL) rupture; mechanical loading was always conducted in the morning. Buprenorphine (0.05 mg kg^{-1}) was administered subcutaneously to mice at the start of the experiment; animals were able to move freely and were monitored for welfare and lameness until termination of the experiment by cervical dislocation. Contralateral limbs, along with limbs from naïve mice served as controls (Gilbert et al., 2018). In total, 18 mice were subjected to ACL rupture (with 6 and 12 euthanised at day 1 and 7 post procedure, respectively). Six mice were naïve controls (Supplemental Figure 1).

Total RNA extraction from mouse medial knee cartilage following DMM

Medial knee cartilage caps were dissected from individual mice (four per time-point) pre- or 42-days post-PTOA induction. Tissue was washed three times with sterile DPBS, placed in

cryogenic vials and immediately frozen in liquid nitrogen. For grinding, the tissue was placed in an autoclaved chamber with a ball (Retsch, Verder Scientific UK Ltd, UK) and 250µl QIAzol lysis reagent (QIAGEN, Manchester, UK). The chambers were transferred to Retsch MM200 mixer mill and tissue ground at vibration frequency of 25 Hz for 90 seconds. To this was added an additional 250µl QIAzol lysis reagent and the mixture transferred to an RNase free tube and incubated at room temperature for 5 minutes. 100µl of chloroform was added and the sample vortexed for 15 s, incubated at room temperature for 10 minutes then centrifuged at 12,500 x *g* at 4^{o}C for 5 minutes. The upper RNA containing aqueous phase was transferred into a new Eppendorf and RNA and miRNA were purified using a mirVana™ miR Isolation Kit (Ambion, ThermoFisher Scientific, Loughborough, UK) followed by DNAse treatment (DNA-free™ DNA Removal Kit, Invitrogen, ThermoFisher Scientific) following the manufacturer's protocol.

Total RNA extraction from mouse femoral condyle knee cartilage following ACL rupture

Femoral condyle cartilage caps were detached from underlying subchondral bone at the tidemark (Gilbert et al., 2018). Cartilage was pooled from mice as described (Supplementary Figure 1) from injured, uninjured (contra-lateral knees), or naïve limbs and immediately snap frozen in liquid nitrogen prior to RNA extraction using TRIzol® reagent according to manufacturer's protocol (ThermoFisher Scientific). Total RNA and miRNA were purified from the TRIzol®-cartilage mixture using a mirVana™ miR Isolation Kit followed by DNAse treatment as above and following the manufacturer's protocol and assessed using a spectrophotometer (Nanodrop 1000, ThermoFisher Scientific) and 2100 Bioanalyzer (Agilent Technologies LDA UK Ltd, Stockport, UK) with A260/280 values between 1.8–2.0 and RIN scores >8, respectively.

Murine knee cartilage RNA sequencing and small RNA analysis

For the DMM RNA-seq, extracted RNA was DNase treated and libraries prepared following Takara SMART-Seq v4 Ultra Low Input RNA kit which incorporates rRNA depletion (Takara BIO Europe SAS, Saint-Germain-en-Laye, France). Libraries from the 4 mice per timepoint were sequenced on an Illumina NovaSeq (Illumina, Cambridge, UK). For the ACL model RNA-seq sequencing libraries were prepared from the pooled samples (Supplementary Figure 1) using the TruSeq Stranded Total RNA with ribo-zero GOLD RNA library prep kit or

the NEB Next Small RNA Library kit (New England Biolabs (UK) Ltd, Hitchin, UK) by Wales Gene Park. The MiSeq Nano system (Illumina) was used to complete a sequencing library quality control after which paired-end sequencing was performed using the Illumina Hi-Seq 2500 (Illumina). For both total RNA sequencing datasets data quality control (QC) was via FastQC (v0.11.9) and reads were quality trimmed with Trimmomatic (0.39) (Bolger et al., 2014). Kallisto (v0.46.1) (Bray et al., 2016) was used for pseudo-alignment against mouse GRCm38 (release 103) transcriptome. Mapped transcript expression estimates were summarised to the gene level using Tximport (v1.14.0) (Soneson et al., 2015). One ACL mRNA sample had <50% RNA-seq read mapping rate with Kallisto so was removed from the subsequent analysis.

For the small RNA-sequencing data of the ACL samples, the nf-core small RNA-seq pipeline (revision 1.1.0) (Lorena et al., 2022) was ran with default parameters except using the flags --genome GRCm38 --protocol 'custom' --three_prime_adapter AGATCGGAAGAGCACACGTCTGAACTCCAGTCAC --mirtrace_protocol illumina. Briefly, this pipeline performed quality control with fastQC (v0.11.9) and mirtrace (v0.11.9), trim galore (0.6.6) adaptor trimming and alignment against the mirbase mature miRNA sequence with bowtie1 (1.3.0) (Langmead et al., 2009) and counted aligned reads with samtools (1.12) (Li et al., 2009).

Principal component analysis was performed using DESeq2 (1.26.0) (Love et al., 2014) normalised and variance stabilised gene expression data. For the DMM mouse model data DESeq2 was used to calculate the log2 fold-change (logFC) and *p*-values with the Wald test.

For both the ACL rupture model mRNA and miRNA count data the gene expression was normalised with edgeR and limma voom (v5.52.2) used to calculate log2 fold-change (logFC) and *p*-values with moderated t-statistics (Ritchie et al., 2015). The duplicateCorrelation method in limma allowed accounting for the samples originating from the same mouse pool. P-values were corrected for multiple testing using the Benjamini and Hochberg method to provide the false discovery rate (FDR).

Gene ontology enrichment was performed using goseq (1.48.0) (Young et al., 2010) with either the up and down regulated sets of significantly differentially expressed genes. Terms with Benjamini–Hochberg (BH) corrected p-values of ≤0.05 were regarded as significant. To identify similar gene expression responses in existing musculoskeletal datasets, pre-processed fold changes were downloaded from the SkeletalVis (Soul et al., 2019) database (https://pgb.liv.ac.uk/shiny/jsoul/skeletalvis/) and compared against the query fold-changes using cosine similarity. The cosine similarity scores (between –1 and 1) were scaled to

zscores (standard deviations from the mean) to allow comparison of transcriptional similarity relative to the background of skeletal cell type transcriptomic responses.

ACL RNA-seq, miRNA-seq and DMM RNA-seq data are available from the National Center for Biotechnology Information Gene Expression Omnibus (NCBI GEO) under accessions GSE232206, GSE232208, and GSE229510, respectively.

For validation of miRNA expression, RNA was reverse-transcribed with Applied Biosystems TaqMan™ MicroRNA Reverse Transcription Kit (Life Technologies, Paisley, UK) and real-time RT-PCR performed with specific TaqMan™ MicroRNA assays (Life Technologies), normalizing to the expression of the snRNA *RNU6B* (U6).

Primary human articular chondrocyte isolation, miR-199a-5p level manipulation, and RNA-sequence analysis

Human articular chondrocyte (HAC) isolation from knee cartilage was performed as previously described (Barter et al., 2015). Tissue was donated by four patients with diagnosed osteoarthritis and undergoing joint replacement surgery (age 59-85; 3 female, 1 male; Supplementary Table 1), with informed consent and ethics committee approval (REC 19/LO/0389). Briefly, macroscopically normal cartilage was removed from the subchondral bone and dissected into ~1mm pieces using scalpel and forceps. Enzymatic digestion was performed using hyaluronidase, trypsin and then collagenase overnight at 37^{o}C (Cleaver et al., 2001). For modulation of miR-199 levels in HAC, Dharmacon miRIDIAN hairpin inhibitor against miR-199a-5p (IH-300607) or Dharmacon miRIDIAN miRNA hairpin inhibitor nontargeting Control #2 (IN-002005-01) were transfected into 40%–50% confluent HAC using Dharmafect 1 lipid reagent (Horizon Discovery, Cambridge, UK) at 100 nM final concentration. Twenty-four hours later RNA was isolated following the miRVana protocol, quality assessed, and cDNA libraries generated using the Illumina TruSeq Stranded mRNA protocol and sequenced on an Illumina NextSeq500 instrument. Kallisto, Tximport and PCA were used for analysis as described above, but with pseudo-alignment to the human GRCh38 (release 103) transcriptome. TargetScanHuman (release 8.0) (McGeary et al., 2019) and mirDIP (Tokar et al., 2018) were used to identify potentially direct targets of miR-199a/b-5p. DESeq2 (1.26.0) was used to calculate the log2 fold-change (logFC) and *p*-values with the Wald test while accounting for the donor origin of each sample. Reactome pathway enrichment analysis was performed using goseq (1.48.0) (Young et al., 2010) with either the up and down regulated sets of differentially expressed genes. Terms with Benjamini–Hochberg (BH) corrected p-values of ≤0.05 were regarded as significant. Data are available at NCBI GEO GSE229437.

Cloning and Plasmid Transfection in SW1353 Cells

miRNA target 3'UTRs were amplified by PCR from human genomic DNA or synthesised as GeneArt DNA fragments (Life Techologies) to enable In-Fusion HD cloning (Takara) into the previously *Xho*I linearized pmirGLO Dual-Luciferase miRNA Target Expression Vector (Promega, Southampton, U.K.) following the manufacturer's instructions (Supplementary Table 2). Mutation of the miRNA seed within the plasmid was performed using the QuikChange II Site-Directed Mutagenesis Kit (Agilent Technologies) or altering the GeneArt DNA fragment sequence synthesized (Supplementary Table 2). All vectors were sequence verified. SW1353 chondrosarcoma cells were cultured in 96-well plates overnight at 50% confluence (1.5×10^4 cells/cm^3). Cells were first transfected with 3'UTR luciferase constructs (10 ng) using FuGENE HD transfection reagent (Promega) for 4 hours then transfected using Dharmafect 1 with Dharmacon miR-199a-5p mimic (50 nM) or miRNA mimic nontargeting Control #2. Twenty-four hours post the second transfection, the cell lysates were assayed for Firefly and Renilla luciferase levels using the Promega Dual-Luciferase Reporter Assay System measured on a GloMax 96 Microplate Luminometer (Promega). Statistical comparisons were performed using a Student's t test.

Code availability

Code to generate the bioinformatics figures is available https://github.com/soulj/OAModelmicroRNA

Results

Differential expression in response to abnormal mechanical loading of the joint

Previously we have reported a reliable and reproducible non-invasive loading model of joint injury with a defined point of injury, ACL rupture following mechanical insult (Gilbert et al., 2018). The model develops with early joint swelling accompanied by an acute inflammatory response followed by joint degeneration, observable histologically as early as 7 days post-ACL rupture. To further characterise this model and define early gene expression changes we performed an unbiased transcriptomics time course early after abnormal mechanical loading and ACL rupture on isolated cartilage from the femoral condyle. Joint injury samples at Day 7 post-injury were distinguishable from Day 1 post-injury samples and naïve and contralateral controls (Figure 1A). No genes were identified as significantly differentially expressed one day post injury (versus naïve) but 2221 and 774 genes (≥1.5-fold, FDR≤0.05) were significantly up and down regulated respectively seven days post-injury (Figure 1B and Supplementary Table 3). Gene ontology enrichment analysis (Figure 1C, Supplementary

Table 4) of the upregulated genes showed alterations in several anabolic terms including 'extracellular matrix organization' (adjusted (adj) p= 1.61E-49), 'chondrocyte differentiation' (adj. p= 1.63E-16), 'Wnt signaling' (adj. p= 3.042E-13), 'Bmp signaling' (adj. p= 1.10E-10) as well as 'response to mechanical stimulus' (adj. p=0.011). In general, pathways were less enriched for the down-regulated genes but included terms related to molecule localisation or transport e.g., 'vesicle-mediated transport' (adj. p= 2.55E-11) along with pathways such as 'response to endoplasmic reticulum stress' (adj. p= 0.0002) and 'catabolic process' (adj. p= 1.10E-06) (Figure 1D, Supplementary Table 4).

We previously curated gene perturbations (genetic or pharmacological) in animal models of joint damage (OATargets; (Soul et al., 2021)) and categorised these genes into those having a 'Protective' (less damage with activation) or a 'Detrimental' (more damage with activation) effect. Amongst the genes upregulated with ACL rupture, those known to alter OA phenotypes when perturbed were primarily protective (68/217 Protective vs 36/199 Detrimental OATarget genes differentially expressed, p=0.002367). These included genes such as *Matn2* (7.87 fold, adj. p= 4.74E-11), *Sulf2* (5.49 fold, adj. p= 3.68E-08), *Loxl2* (7.18 fold, adj. p=4.55E-09), *Gdf5* (14.80 fold, adj. p= 4.11E-07), and *Sox9* (2.57 fold, adj. p= 4.69E-05), suggestive of an anabolic transcriptomic response to the abnormal mechanical load (Figure 1E). Upregulated known detrimental OATarget genes in the ACL model at Day 7 included the protease *Htra1* (5.06 fold, adj. p= 2.60E-08), *Adamts7* (3.14 fold, adj. p= 5.58E-07), *Postn* (21.76 fold, adj. p= 3.91E-07), *Acvr1* (2.49 fold, adj. p= 1.12E-06), *Atf3* (2.59 fold, adj. p= 3.23E-05) and the mechanical activated kinase *Fyn* (1.31 fold, adj. p= 0.012). Comparable gene expression results were observed versus contralateral controls (Supplementary Table 3).

To validate our transcriptomics data, we next compared the Day 7 ACL rupture model gene expression responses to the SkeletalVis database of 800 transcriptional responses from skeletal cell types (Soul et al., 2019). This analysis allowed assessment of the most similar gene expression responses (log2 fold changes) from a large database of potentially relevant datasets. Similarity between pairs of log2 fold changes were calculated using cosine similarity, where similar fold changes received positive scores and opposite fold changes received negative scores. These scores were then converted to zscores (standard deviations from the mean similarity) to facilitate comparison across all datasets. Among the most similar were several other post-traumatic joint injury responses including DMM and ACLT (surgical transection of the ACL) from a range of time points, suggesting these generated data from the abnormal loading model share common features with other models of PTOA (Figure 1F, Table 1, Supplementary Table 5). Interestingly, mouse knockout of the known chondrogenesis inhibitor *Frzb* was found to induce a similar transcriptomic response.

These data suggest a predominantly chondroprotective expression response in the joint shortly after abnormal mechanical loading.

Next, we directly assessed if the gene expression changes seen in the ACL model were comparable to those from later time points of the DMM model where similar levels of joint degeneration are observed (Gilbert et al., 2018; Glasson et al., 2007). We therefore performed RNA-seq on RNA from medial knee cartilage caps dissected from individual mice pre- and day 42 post-DMM surgery. By principal component analysis (PCA) the different groups were clearly distinguishable (Figure 2A). In all, we detected 2063 genes differentially expressed (≥1.5-fold, FDR≤0.05) with 1167 and 896 up and down-regulated, respectively (Figure 2B, Supplementary Table 6). Gene ontology enrichment analysis (Figure 2C, Supplementary Table 7) of the upregulated genes showed alterations in several anabolic terms including 'extracellular matrix organisation' (adj. p=5.78E-047) and 'response to wounding' (adj. p= 1.5E-07). The down-regulated genes were enriched in those within cell cycle terms (Figure 2D, Supplementary Table 7). Again, in the up-regulated gene list, those known to alter OA phenotypes when perturbed were mainly protective (53/200 Protective vs 22/181 Detrimental OATarget genes differentially expressed, p=0.00053) and similar to those described for the ACL-rupture model (Figure 2E). Direct comparison of the differentially expressed genes between the ACL and DMM model showed a strong correlation (Spearman R =0.82, P<2.2E-16) (Figure 2F), with <2% of differentially expressed genes regulated in opposing directions, again indicating the shared transcriptomic responses in these PTOA models. No gene ontology terms were enriched for these non-concordant genes.

miRNA differential expression analysis

Having characterised the mRNA expression profiles of the ACL rupture model we next sought to identify potential post-transcriptional regulators of the observed differential expression. We performed small RNA sequencing to characterise the miRNA response to acute joint injury using the naïve, contralateral and ACL rupture femoral condyle cartilage cap samples described previously. PCA again suggested the naïve and contralateral limb had similar miRNA profiles with only the ACL rupture model mice being distinguishable 7 days after mechanical insult (Figure 3A). Similar to the mRNA-sequencing, no significant differential expression was observed at one day post-insult. Sixty-three statistically significant upregulated and 16 downregulated miRNAs were identified 7 days post mechanical loading (Day 7 ACL versus naïve; Figure 3B and Supplementary Table 8). Highly abundant, significantly differentially expressed miRNAs included miR-199a/b-3p (2.2

fold, adj. p=0.00285), miR-199a-5p (2.21 fold, adj. p=0.00144) and previously reported mechanosensitive miRNAs miR-27b-3p (1.56 fold, adj. p=0.0316) and miR-21a- 5p (3.5 fold, adj. p=0.000129) (Figure 3B). miR-199a-5p and miR-21a-5p were also found to be upregulated in cartilage following DMM surgery (Figure 3C).

Characterisation of miR-199-5p in human osteoarthritic chondrocytes

Among the highly abundant differentially expressed miRNAs identified in both the ACL and DMM models we have recently reported the role of miR-199a-5p as a positive regulator of human MSC chondrogenesis (Patel et al., 2023). Moreover, intra-articular delivery of the miRNA has also been shown to exert a significant protective effect in rat OA model (Huang et al., 2023). Thus, we sought to further understand the most responsive potential targets of miR-199a-5p in a human OA chondrocyte context. RNA-sequencing after miR-199a-5p inhibition (Supplementary Figure 2) in primary human articular chondrocytes from four donors showed differential expression of 133 up and 113 down-regulated genes (Figure 4A and Supplementary Table 9). Chondrocyte maturation associated genes such as *MMP1* (1.63 fold, adj. p=3.85E-10), *MMP13* (1.28 fold, adj. p=0.0003), *BMP2* (1.4 fold, adj. p= 5.5E-10), *INHBA* (activin-A) (1.48 fold, adj. p=1.4E-07), *SPP1* (Osteopontin) (1.45 fold, adj. p=11.1E-06) and *COMP* (-1.35 fold, adj. p=3.25E-05) were differentially expressed suggesting a role for miR-199a-5p in regulating the chondrocyte phenotype. The host gene for *MIR199A*, *DNM3OS*, was also upregulated (1.31 fold, adj. p=0.0024) suggesting some autoregulation. Gene ontology enrichment analysis showed significant enrichment of ‘extracellular matrix organisation’ (adj. p= 0.00663) and ‘G1 DNA damage checkpoint’ (adj. p= 0.0418) (Figure 4B,Supplementry Table 10). We also inhibited miR-199b-5p however, we were unable to confirm selective miRNA inhibition (Supplementary Figure 2). Regardless, both miRNAs contain the same seed sequence (5’ nucleotides 2-8) (Kozomara et al., 2019), so unsurprisingly strong correlation of the fold changes (Spearman’s correlation coefficient = 0.89, p-value= 2.2E-16) was observed (Supplementary Table 9). Genes significantly upregulated by miR-199b-5p inhibition, also elevated in the miR-199a-5p inhibition dataset, included the described *MMP1*, *MMP13* and *BMP2*.

Comparison of the gene expression response to other responses in SkeletalVis showed miR-199a-5p inhibition resulted in an expression profile most similar to the overexpression of the transcription factor TBX5 (zscore=3.62), human OA damaged vs intact cartilage (zscore=3.43) and murine cartilage 6 weeks post DMM-surgery (WT DMM 6wkvsWT Sham 6wk) cartilage (zscore=3.19) suggesting that miR-199a-5p depletion induces a similar expression profile to that seen in damaged OA cartilage (Supplementary Table 11).

Of the 133 genes significantly increased in expression following miR-199a-5p inhibition, 19 were TargetScan predicted targets of the miRNA (Figure 4C). This is a significant (p=0.0004) enrichment given there was only 1 predicted target in the 113 down-regulated genes. We also explored comprehensive predictions from the mirDIP target prediction database (Tokar et al., 2018), which identified of a further 14 miR-199a-5p target genes within the 133 up-regulated gene list. The up-regulated genes included experimentally validated targets of miR-199a-5p such as *FZD6* (1.79 fold, adj. p=9.93E-23) (Kim et al., 2015) but also several less well described targets such as *ECE1* (1.72 fold, adj. p=1.79E-12), *SOS2* (1.46 fold, adj. p= 2.81E-09), *CELSR1* (1.38 fold, adj. p=0.0011) *GIT1* (1.25 fold, adj. p=0.0176), and *SLC9A8* (1.27 fold, adj. p=0.000242). Interestingly, of those predicted miR-199a-5p targets increased in expression upon inhibition of the miRNA in OA chondrocytes, a significant proportion (p<0.02) were also increased in our murine ACL data. Finally, we tested whether these genes were direct targets of miR-199a-5p using dual-luciferase reporter assays. 3'UTR containing luciferase plasmids were co-transfected with control or miR-199a-5p mimics into the SW1353 chondrosarcoma cell line. From these, *CELSR1*, *GIT1*, *ECE1* and *SOS2* were repressed by the miR-199a-5p mimic. This repression was lost by mutation of the predicted miRNA binding sequence within each 3'UTR (Figure 4D).

Discussion

Our primary aim in this study was to define the early transcriptomic response of cartilage to mechanical damage in a nonsurgical, highly reproducible, ACL rupture model. The non-surgical ACL rupture model transcriptomic signature was highly correlative with our own and published data from the well-established DMM OA model this was despite the limitations of study experimental design (Supplementary Figure 1) and in that we did not assess the transcriptional aspect of the ACL model at an identical time point to the DMM. The ACL rupture model is a rapidly progressing OA model and at day 7, significant cartilage damage is observed histologically; typically by day 21 the cartilage has eroded completely (Gilbert et al., 2018), thus the day 7 time point is more comparable and better reflects the extent of degeneration observed in the DMM model at day 42 (Glasson et al., 2007). Transcriptome assessment of early time-points of the DMM model are confounded by the effects of surgery, as determined through the use of sham surgeries (Bateman et al., 2013; Loeser et al., 2013). This highlights one benefit of the mechanically-induced, non-surgical, ACL rupture model over that of DMM, in that it obviates the need for sham surgeries as the transcriptomic signature of the contralateral limb was equivalent to that of naïve animals, thus reducing animal numbers required to achieve power in a study.. The ACL model also better replicates

a traumatic injury experienced by humans allowing the study of early biological joint changes for the development of potential therapeutic interventions (Christiansen et al., 2015).The data presented here highlights the usefulness of the ACL rupture model as a non-invasive, highly reproducible, alternative or companion to the DMM model. What was clear from both the DMM and particularly the ACL datasets was that the transcriptomic response to injury also involved repair activation. This included enrichment for pathways such as 'extracellular matrix organization' and 'cellular response to growth factor stimulus'. Up-regulated genes in both datasets contained several collagen genes as well as the predicted proteases, especially of the MMP family. In fact, others have reported that following injury in a PTOA model there is a distinct anabolic response, possibly mediated by the injured synovial tissue (Knights et al., 2023; Lai-Zhao et al., 2021).

We also performed small RNA-seq following ACL rupture, defining miRNAs differentially and most abundantly expressed, which included miR-27b-3p, miR-21a-5p and both the 5p and 3p arms from miR-199. Both miR-21 and miR-27 are known mechano-regulated miRNAs and we have previously reported their regulation following the loading of *ex vivo* cartilage explants (Stadnik et al., 2021). In vivo, loss of miR-21a-5p alleviates cartilage matrix degradation in a murine temporomandibular joint OA model (Zhang et al., 2020); while intra-articular injection of a miR-27-3p agomir/mimic contributes to a synovial fibrotic response in murine knee OA, though injection of an inhibitor of the miRNA did not alter DMM-induced OA progression (Tavallaee et al., 2022).

MiRNA-199 is present at three locations in the human genome, antisense within an intron of a Dynamin (DNM) gene.The 3p arms of the miRNA are identical and are generally the most abundantly expressed, though the 5p arms are also readily detectible. miR-199b-5p differs slightly in sequence from the miR-199a-5p's though in all cases the seed sequence (5' nucleotides 2-8) are identical (Kozomara et al., 2019). Mir-199a-2 is part of a miRNA cluster with miR-214 and miR-3120 and though present in an intron of *DNM3* the cluster are actually located within the long non-coding RNA (lncRNA) *DNM3OS* on human chromosome 1q24 (Shepherdson et al., 2021). Patients with small deletions of this chromosomal region affecting *DNM3OS* and the incumbent miRNAs have skeletal abnormalities which include short stature, microcephaly, and brachydactyly (Lefroy et al., 2018), somewhat phenocopied by the deletion of *Dnm3os*, and therefore the miR199a~214 cluster, in mice (Watanabe et al., 2008).

Several studies have addressed miR-199 in the context of cartilage or OA ((Akhtar and Haqqi, 2012; Ali et al., 2020; Chao et al., 2020; Prasadam et al., 2016). , In rodents with surgically-induced OA, serum levels of miR-199a-5p increased (Lu et al., 2022), as we observed in cartilage following PTOA induction. The source of miR-199a-5p in serum is unclear, but inhibition of miR-199a-5p via intra-articular injection of an antagomir following OA induction in rats reportedly decreased joint inflammation and reduced cytokine levels (Lu et al., 2022). This observation is contradictory to the intra-articular injection of a mimic (agomir) miR-199a-5p which reduced cartilage damage in a rat PTOA model (Huang et al., 2023).

Given the conflicting literature surrounding miR-199a-5p, we chose to manipulate the levels of the miRNA in cultured primary chondrocytes using inhibition with a specific hairpin Inhibitor, since both physiological and supraphysiological overexpression of miRNA mimics can lead to spurious findings (Jin et al., 2015). Our RNA-seq analysis revealed that miR-199a/b-5p inhibition led to a transcriptome response similar to that of both human OA damaged vs intact cartilage and murine DMM cartilage six weeks post-surgery. This included the upregulation of the destructive collagenases, *MMP1* and *MMP13*. Thus, we would predict that the increase in miR-199a-5p observed following PTOA induction *in vivo* is part of a chondroprotective response to the abnormal mechanical load experienced by the animal, in line with the overexpression of miR-199a-5p *in vivo* reducing histological joint damage and Mmp13 expression (Huang et al., 2023).

Overall, predicted targets of miR-199 were significantly enriched in the upregulated gene set following miR-199a/b-5p inhibition. Amongst these were *FZD6*, a receptor involved in WNT signalling. *FZD6* has previously been reported as a miR-199a-5p target (Kim et al., 2015), but interestingly is also a target of another important cartilage miRNA, miR-140-5p (Kim et al., 2015). Although WNT signalling has been extensively studied in cartilage development and OA (De Palma and Nalesso, 2021), little information pertains to a direct role for FZD6 in the tissue. Other direct targets of miR-199a-5p confirmed in this study include *GIT1*, *CELSR1*, *SOS2* and *ECE1*, the latter of which has previously been validated (Bao et al., 2018).

Several studies have profiled miRNAs in PTOA models. By small RNA-seq Castanheira *et al.*, (Castanheira et al., 2021) identified just four miRNAs as differentially expressed 8-weeks post DMM surgery. None of these miRNAs were significantly changed in our ACL rupture model which may reflect the different models, but is more likely due to different sampling, with the authors isolating RNA from whole mouse joints not just articular cartilage . Kung *et al*., (Kung et al., 2018) also profiled miRNAs in dissected cartilage during DMM OA-

induction. At six weeks post-surgery they identified 74 differentially expressed miRNAs, ten of which are also differentially expressed in our 7-day post ACL rupture data. However, only 3 miRNAs (miR-31-5p, miR486a-5p and miR-10a-5p) share the same direction of expression change. The lack of correlation between our ACL and the published DMM miRNA datasets is surprising, especially given our finding that gene expression at day 7-post ACL and day 42-post DMM are highly correlative. Both experimental designs were similar, with approximately equal sample numbers and the use of pooled animals. The main difference is the technology used, small RNA-seq herein versus microarray (Kung et al., 2018). We did not perform small RNA-seq following DMM, which would be valuable, however in our DMM cartilage RNA we were also able to confirm the up-regulation of miR-199a-5p and miR-21a-5p by real-time PCR , validating our ACL miRNA profile and supporting a role for these miRNAs in cartilage tissue integrity.

In conclusion, here we further characterise the ACL rupture model providing for the first time both mRNA and miRNA-seq data. The transcriptomic response of the DMM and ACL-rupture PTOA models were highly correlative. This, when added with the ACL-rupture models relative simplicity, speed, reproducibility, and no requirement for sham animals, means it could be valuable in medium throughput PTOA perturbation studies. The PTOA miRNA signature has confirmed the upregulation of numerous miRNAs including those known to be regulated by altered biomechanical load. We also identified miR-199a-5p as being abundantly expressed and increased in both PTOA models. Inhibition of this miRNA in primary human chondrocytes gave a transcriptome profile with similarity to human OA damaged vs intact cartilage and murine DMM. Further work will be needed to resolve the role miR-199 and its differing forms have in OA *in vivo*.

Acknowledgments

No writing assistance was obtained for this article.

Author contributions

Conception and design: SJG, KAP, EJB, JS, DAY

Collection and assembly of data: SJG, EJB, HL, YH, KAP, JC, KP and MJB

Analysis and interpretation of the data: SJG, EJB, JS, MJB and DAY

Drafting of the article: SJG, EJB, JS, DAY

Obtaining of funding: EJB and DAY

Final approval of the article: All authors

Role of the funding source

This study was funded by Versus Arthritis grant 18461 (SJG, EJB) and 22043 (DAY); the Medical Research Council and Versus Arthritis as part of the MRC-Arthritis Research UK Centre for Integrated Research into Musculoskeletal Ageing (CIMA) (JXR 10641, MR/P020941/1); the JGW Patterson Foundation; and The Dunhill Medical Trust (R476/0516). The study sponsors were not involved in any aspect of the study.

Competing interests

All authors declare no conflicts of interest.

References

Akhtar, N. and Haqqi, T. M. (2012). MicroRNA-199a* regulates the expression of cyclooxygenase-2 in human chondrocytes. *Ann Rheum Dis* **71**, 1073-80.

Ali, S. A., Gandhi, R., Potla, P., Keshavarzi, S., Espin-Garcia, O., Shestopaloff, K., Pastrello, C., Bethune-Waddell, D., Lively, S., Perruccio, A. V. et al. (2020). Sequencing identifies a distinct signature of circulating microRNAs in early radiographic knee osteoarthritis. *Osteoarthritis Cartilage* **28**, 1471-1481.

Bao, N., Fang, B., Lv, H., Jiang, Y., Chen, F., Wang, Z. and Ma, H. (2018). Upregulation of miR-199a-5p Protects Spinal Cord Against Ischemia/Reperfusion-Induced Injury via Downregulation of ECE1 in Rat. *Cell Mol Neurobiol* **38**, 1293-1303.

Bartel, D. P. (2009). MicroRNAs: target recognition and regulatory functions. *Cell* **136**, 215-33.

Barter, M. J., Tselepi, M., Gomez, R., Woods, S., Hui, W., Smith, G. R., Shanley, D. P., Clark, I. M. and Young, D. A. (2015). Genome-Wide MicroRNA and Gene Analysis of Mesenchymal Stem Cell Chondrogenesis Identifies an Essential Role and Multiple Targets for miR-140-5p. *Stem Cells* **33**, 3266-80.

Bateman, J. F., Rowley, L., Belluoccio, D., Chan, B., Bell, K., Fosang, A. J. and Little, C. B. (2013). Transcriptomics of wild-type mice and mice lacking ADAMTS-5 activity identifies genes involved in osteoarthritis initiation and cartilage destruction. *Arthritis Rheum* **65**, 1547-60.

Blaker, C. L., Clarke, E. C. and Little, C. B. (2017). Using mouse models to investigate the pathophysiology, treatment, and prevention of post-traumatic osteoarthritis. *J Orthop Res* **35**, 424-439.

Bolger, A. M., Lohse, M. and Usadel, B. (2014). Trimmomatic: a flexible trimmer for Illumina sequence data. *Bioinformatics* **30**, 2114-20.

Bray, N. L., Pimentel, H., Melsted, P. and Pachter, L. (2016). Near-optimal probabilistic RNA-seq quantification. *Nat Biotechnol* **34**, 525-7.

Brown, T. D., Johnston, R. C., Saltzman, C. L., Marsh, J. L. and Buckwalter, J. A. (2006). Posttraumatic osteoarthritis: a first estimate of incidence, prevalence, and burden of disease. *J Orthop Trauma* **20**, 739-44.

Burleigh, A., Chanalaris, A., Gardiner, M. D., Driscoll, C., Boruc, O., Saklatvala, J. and Vincent, T. L. (2012). Joint immobilization prevents murine osteoarthritis and reveals the highly mechanosensitive nature of protease expression in vivo. *Arthritis Rheum* **64**, 2278-88.

Castanheira, C., Anderson, J. R., Fang, Y., Milner, P. I., Goljanek-Whysall, K., House, L., Clegg, P. D. and Peffers, M. J. (2021). Mouse microRNA signatures in joint ageing and post-traumatic osteoarthritis. *Osteoarthr Cartil Open* **3**, 100186.

Chang, J. C., Sebastian, A., Murugesh, D. K., Hatsell, S., Economides, A. N., Christiansen, B. A. and Loots, G. G. (2017). Global molecular changes in a tibial compression induced ACL rupture model of post-traumatic osteoarthritis. *J Orthop Res* **35**, 474-485.

Chao, Y., Zhang, L., Zhang, X., Ma, C. and Chen, Z. (2020). Expression of MiR-140 and MiR-199 in Synovia and its Correlation with the Progression of Knee Osteoarthritis. *Med Sci Monit* **26**, e918174.

Christiansen, B. A., Guilak, F., Lockwood, K. A., Olson, S. A., Pitsillides, A. A., Sandell, L. J., Silva, M. J., van der Meulen, M. C. and Haudenschild, D. R. (2015). Non-invasive mouse models of post-traumatic osteoarthritis. *Osteoarthritis Cartilage* **23**, 1627-38.

Cleaver, C. S., Rowan, A. D. and Cawston, T. E. (2001). Interleukin 13 blocks the release of collagen from bovine nasal cartilage treated with proinflammatory cytokines. *Ann Rheum Dis* **60**, 150-7.

De Palma, A. and Nalesso, G. (2021). WNT Signalling in Osteoarthritis and Its Pharmacological Targeting. *Handb Exp Pharmacol* **269**, 337-356.

Garriga, C., Goff, M., Paterson, E., Hrusecka, R., Hamid, B., Alderson, J., Leyland, K., Honeyfield, L., Greenshields, L., Satchithananda, K. et al. (2021). Clinical and molecular associations with outcomes at 2 years after acute knee injury: a longitudinal study in the Knee Injury Cohort at the Kennedy (KICK). *Lancet Rheumatol* **3**, e648-e658.

Gelber, A. C., Hochberg, M. C., Mead, L. A., Wang, N. Y., Wigley, F. M. and Klag, M. J. (2000). Joint injury in young adults and risk for subsequent knee and hip osteoarthritis. *Ann Intern Med* **133**, 321-8.

Gilbert, S. J., Bonnet, C. S., Stadnik, P., Duance, V. C., Mason, D. J. and Blain, E. J. (2018). Inflammatory and degenerative phases resulting from anterior cruciate rupture in a non-invasive murine model of post-traumatic osteoarthritis. *J Orthop Res*.

Glasson, S. S., Blanchet, T. J. and Morris, E. A. (2007). The surgical destabilization of the medial meniscus (DMM) model of osteoarthritis in the 129/SvEv mouse. *Osteoarthritis Cartilage* **15**, 1061-9.

Huang, L., Jin, M., Gu, R., Xiao, K., Lu, M., Huo, X., Sun, M., Yang, Z., Wang, Z., Zhang, W. et al. (2023). miR-199a-5p Reduces Chondrocyte Hypertrophy and Attenuates Osteoarthritis Progression via the Indian Hedgehog Signal Pathway. *J Clin Med* **12**.

Jin, H. Y., Gonzalez-Martin, A., Miletic, A. V., Lai, M., Knight, S., Sabouri-Ghomi, M., Head, S. R., Macauley, M. S., Rickert, R. C. and Xiao, C. (2015). Transfection of microRNA Mimics Should Be Used with Caution. *Front Genet* **6**, 340.

Kilkenny, C., Browne, W. J., Cuthill, I. C., Emerson, M. and Altman, D. G. (2012). Improving bioscience research reporting: the ARRIVE guidelines for reporting animal research. *Osteoarthritis Cartilage* **20**, 256-60.

Kim, B. K., Yoo, H. I., Kim, I., Park, J. and Kim Yoon, S. (2015). FZD6 expression is negatively regulated by miR-199a-5p in human colorectal cancer. *BMB Rep* **48**, 360-6.

Knights, A. J., Farrell, E. C., Ellis, O. M., Lammlin, L., Junginger, L. M., Rzeczycki, P. M., Bergman, R. F., Pervez, R., Cruz, M., Knight, E. et al. (2023). Synovial fibroblasts assume distinct functional identities and secrete R-spondin 2 in osteoarthritis. *Ann Rheum Dis* **82**, 272-282.

Kozomara, A., Birgaoanu, M. and Griffiths-Jones, S. (2019). miRBase: from microRNA sequences to function. *Nucleic Acids Res* **47**, D155-D162.

Kung, L. H., Zaki, S., Ravi, V., Rowley, L., Smith, M. M., Bell, K. M., Bateman, J. F. and Little, C. B. (2017a). Utility of circulating serum miRNAs as biomarkers of early cartilage degeneration in animal models of post-traumatic osteoarthritis and inflammatory arthritis. *Osteoarthritis Cartilage* **25**, 426-434.

Kung, L. H. W., Ravi, V., Rowley, L., Angelucci, C., Fosang, A. J., Bell, K. M., Little, C. B. and Bateman, J. F. (2018). Cartilage MicroRNA Dysregulation During the Onset and Progression of Mouse Osteoarthritis Is Independent of Aggrecanolysis and Overlaps With Candidates From End-Stage Human Disease. *Arthritis Rheumatol* **70**, 383-395.

Kung, L. H. W., Ravi, V., Rowley, L., Bell, K. M., Little, C. B. and Bateman, J. F. (2017b). Comprehensive Expression Analysis of microRNAs and mRNAs in Synovial Tissue from a Mouse Model of Early Post-Traumatic Osteoarthritis. *Sci Rep* **7**, 17701.

Lai-Zhao, Y., Pitchers, K. K. and Appleton, C. T. (2021). Transient anabolic effects of synovium in early post-traumatic osteoarthritis: a novel ex vivo joint tissue co-culture system for investigating synovium-chondrocyte interactions. *Osteoarthritis Cartilage* **29**, 1060-1070.

Langmead, B., Trapnell, C., Pop, M. and Salzberg, S. L. (2009). Ultrafast and memory-efficient alignment of short DNA sequences to the human genome. *Genome Biol* **10**, R25.

Lefroy, H., Fox, O., Javaid, M. K., Makaya, T. and Shears, D. J. (2018). 1q24 deletion syndrome. Two cases and new insights into genotype-phenotype correlations. *Am J Med Genet A* **176**, 2004-2008.

Li, H., Handsaker, B., Wysoker, A., Fennell, T., Ruan, J., Homer, N., Marth, G., Abecasis, G., Durbin, R. and Genome Project Data Processing, S. (2009). The Sequence Alignment/Map format and SAMtools. *Bioinformatics* **25**, 2078-9.

Lieberthal, J., Sambamurthy, N. and Scanzello, C. R. (2015). Inflammation in joint injury and post-traumatic osteoarthritis. *Osteoarthritis Cartilage* **23**, 1825-34.

Loeser, R. F., Olex, A. L., McNulty, M. A., Carlson, C. S., Callahan, M., Ferguson, C. and Fetrow, J. S. (2013). Disease progression and phasic changes in gene expression in a mouse model of osteoarthritis. *PLoS One* **8**, e54633.

Lohmander, L. S., Englund, P. M., Dahl, L. L. and Roos, E. M. (2007). The long-term consequence of anterior cruciate ligament and meniscus injuries: osteoarthritis. *Am J Sports Med* **35**, 1756-69.

Lorena, P., Phil, E., Chuan, W., Jose, E.-C., Kevin, M., Alexander, P., Icabus, f., Kevin, nf-core, b. and Harshil, P. (2022). nf-core/smrnaseq: v 2.0.0 - 2022-05-31 Aqua Zinc Chihuahua.

Love, M. I., Huber, W. and Anders, S. (2014). Moderated estimation of fold change and dispersion for RNA-seq data with DESeq2. *Genome Biol* **15**, 550.

Lu, H., Yang, Y., Ou, S., Qi, Y., Li, G., He, H., Lu, F., Li, W. and Sun, H. (2022). The silencing of miR-199a-5p protects the articular cartilage through MAPK4 in osteoarthritis. *Ann Transl Med* **10**, 601.

McGeary, S. E., Lin, K. S., Shi, C. Y., Pham, T. M., Bisaria, N., Kelley, G. M. and Bartel, D. P. (2019). The biochemical basis of microRNA targeting efficacy. *Science* **366**.

Muthuri, S. G., McWilliams, D. F., Doherty, M. and Zhang, W. (2011). History of knee injuries and knee osteoarthritis: a meta-analysis of observational studies. *Osteoarthritis Cartilage* **19**, 1286-93.

Narez, G. E., Fischenich, K. M. and Donahue, T. L. H. (2020). Experimental animal models of post-traumatic osteoarthritis of the knee. *Orthop Rev (Pavia)* **12**, 8448.

Neuman, P., Englund, M., Kostogiannis, I., Friden, T., Roos, H. and Dahlberg, L. E. (2008). Prevalence of tibiofemoral osteoarthritis 15 years after nonoperative treatment of anterior cruciate ligament injury: a prospective cohort study. *Am J Sports Med* **36**, 1717-25.

Patel, K., Barter, M. J., Soul, J., Proctor, C. J., Clark, I. M., Young, D. A. and Shanley, D. P. (2023). Systems analysis of miR-199a/b-5p and multiple miR-199a/b-5p targets during chondrogenesis. *bioRxiv*.

Peat, G., Bergknut, C., Frobell, R., Joud, A. and Englund, M. (2014). Population-wide incidence estimates for soft tissue knee injuries presenting to healthcare in southern Sweden: data from the Skane Healthcare Register. *Arthritis Res Ther* **16**, R162.

Prasadam, I., Batra, J., Perry, S., Gu, W., Crawford, R. and Xiao, Y. (2016). Systematic Identification, Characterization and Target Gene Analysis of microRNAs Involved in Osteoarthritis Subchondral Bone Pathogenesis. *Calcif Tissue Int* **99**, 43-55.

Sanders, T. L., Maradit Kremers, H., Bryan, A. J., Larson, D. R., Dahm, D. L., Levy, B. A., Stuart, M. J. and Krych, A. J. (2016). Incidence of Anterior Cruciate Ligament Tears and Reconstruction: A 21-Year Population-Based Study. *Am J Sports Med* **44**, 1502-7.

Scott, K. M., Cohen, D. J., Hays, M., Nielson, D. W., Grinstaff, M. W., Lawson, T. B., Snyder, B. D., Boyan, B. D. and Schwartz, Z. (2021). Regulation of inflammatory and catabolic responses to IL-1beta in rat articular chondrocytes by microRNAs miR-122 and miR-451. *Osteoarthritis Cartilage* **29**, 113-123.

Shepherdson, J. L., Zheng, H., Amarillo, I. E., McAlinden, A. and Shinawi, M. (2021). Delineation of the 1q24.3 microdeletion syndrome provides further evidence for the potential role of non-coding RNAs in regulating the skeletal phenotype. *Bone* **142**, 115705.

Snoeker, B., Turkiewicz, A., Magnusson, K., Frobell, R., Yu, D., Peat, G. and Englund, M. (2020). Risk of knee osteoarthritis after different types of knee injuries in young adults: a population-based cohort study. *Br J Sports Med* **54**, 725-730.

Soneson, C., Love, M. I. and Robinson, M. D. (2015). Differential analyses for RNA-seq: transcript-level estimates improve gene-level inferences. *F1000Res* **4**, 1521.

Soul, J., Barter, M. J., Little, C. B. and Young, D. A. (2021). OATargets: a knowledge base of genes associated with osteoarthritis joint damage in animals. *Ann Rheum Dis* **80**, 376-383.

Soul, J., Hardingham, T. E., Boot-Handford, R. P. and Schwartz, J. M. (2019). SkeletalVis: an exploration and meta-analysis data portal of cross-species skeletal transcriptomics data. *Bioinformatics* **35**, 2283-2290.

Stadnik, P. S., Gilbert, S. J., Tarn, J., Charlton, S., Skelton, A. J., Barter, M. J., Duance, V. C., Young, D. A. and Blain, E. J. (2021). Regulation of microRNA-221, -222, -21 and -27 in articular cartilage subjected to abnormal compressive forces. *J Physiol* **599**, 143-155.

Tavallaee, G., Lively, S., Rockel, J. S., Ali, S. A., Im, M., Sarda, C., Mitchell, G. M., Rossomacha, E., Nakamura, S., Potla, P. et al. (2022). Contribution of MicroRNA-27b-3p to Synovial Fibrotic Responses in Knee Osteoarthritis. *Arthritis Rheumatol* **74**, 1928-1942.

Tokar, T., Pastrello, C., Rossos, A. E. M., Abovsky, M., Hauschild, A. C., Tsay, M., Lu, R. and Jurisica, I. (2018). mirDIP 4.1-integrative database of human microRNA target predictions. *Nucleic Acids Res* **46**, D360-D370.

Watanabe, T., Sato, T., Amano, T., Kawamura, Y., Kawamura, N., Kawaguchi, H., Yamashita, N., Kurihara, H. and Nakaoka, T. (2008). Dnm3os, a non-coding RNA, is required for normal growth and skeletal development in mice. *Dev Dyn* **237**, 3738-48.

Watt, F. E., Paterson, E., Freidin, A., Kenny, M., Judge, A., Saklatvala, J., Williams, A. and Vincent, T. L. (2016). Acute Molecular Changes in Synovial Fluid Following Human Knee Injury: Association With Early Clinical Outcomes. *Arthritis Rheumatol* **68**, 2129-40.

Young, M. D., Wakefield, M. J., Smyth, G. K. and Oshlack, A. (2010). Gene ontology analysis for RNA-seq: accounting for selection bias. *Genome Biol* **11**, R14.

Zhang, G., Zhou, Y., Su, M., Yang, X. and Zeng, B. (2020). Inhibition of microRNA-27b-3p relieves osteoarthritis pain via regulation of KDM4B-dependent DLX5. *Biofactors* **46**, 788-802.

Figures and Tables

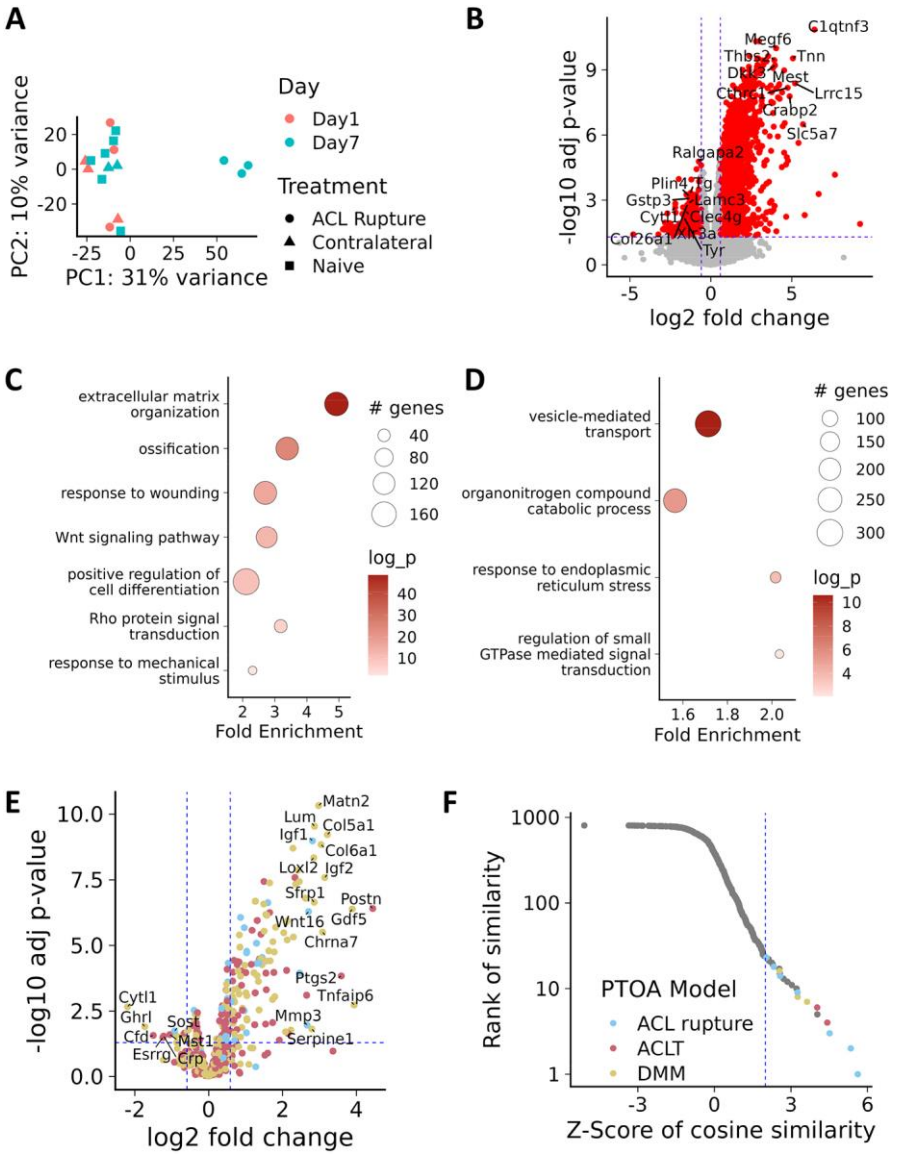

Fig. 1. Protective gene expression in early time points of abnormal mechanical loading following ACL rupture

(**A**) Principal component analysis plots of RNA-seq data from ACL model of post-traumatic osteoarthritis. (**B**) Volcano plot showing differential expression of all genes, red indicate those significantly differentially expressed. Vertical blue lines indicate 1.5-fold change, horizontal - adjusted p-value <0.05. Pathway enrichment plots of the enriched gene ontology terms for the significantly up (**C**) and down-regulated (**D**) genes. Selected gene ontology terms depicted. As indicated circle size represents

the number of genes, the colour intensity depicts the fold enrichment -$\log_{10}$ p value (log_p). (**E**) Volcano plot of expression of known OA affecting genes from Day 7 ACL vs Naïve control. Genes which have detrimental, protective, and ambiguous effects on OA are shown in yellow, red, and blue, respectively. Vertical blue lines indicate 1.5-fold change, horizontal - adjusted p-value <0.05. (**F**) Graph of the rank and value of the Cosine similarity zscores for the comparison of the Day 7 ACL vs Naïve control data with approximately 800 datasets collated in SkeletalVis. The most similar profiles that correspond to PTOA models are highlighted and detailed in Table 1. Coloured points indicate murine PTOA models as labelled.

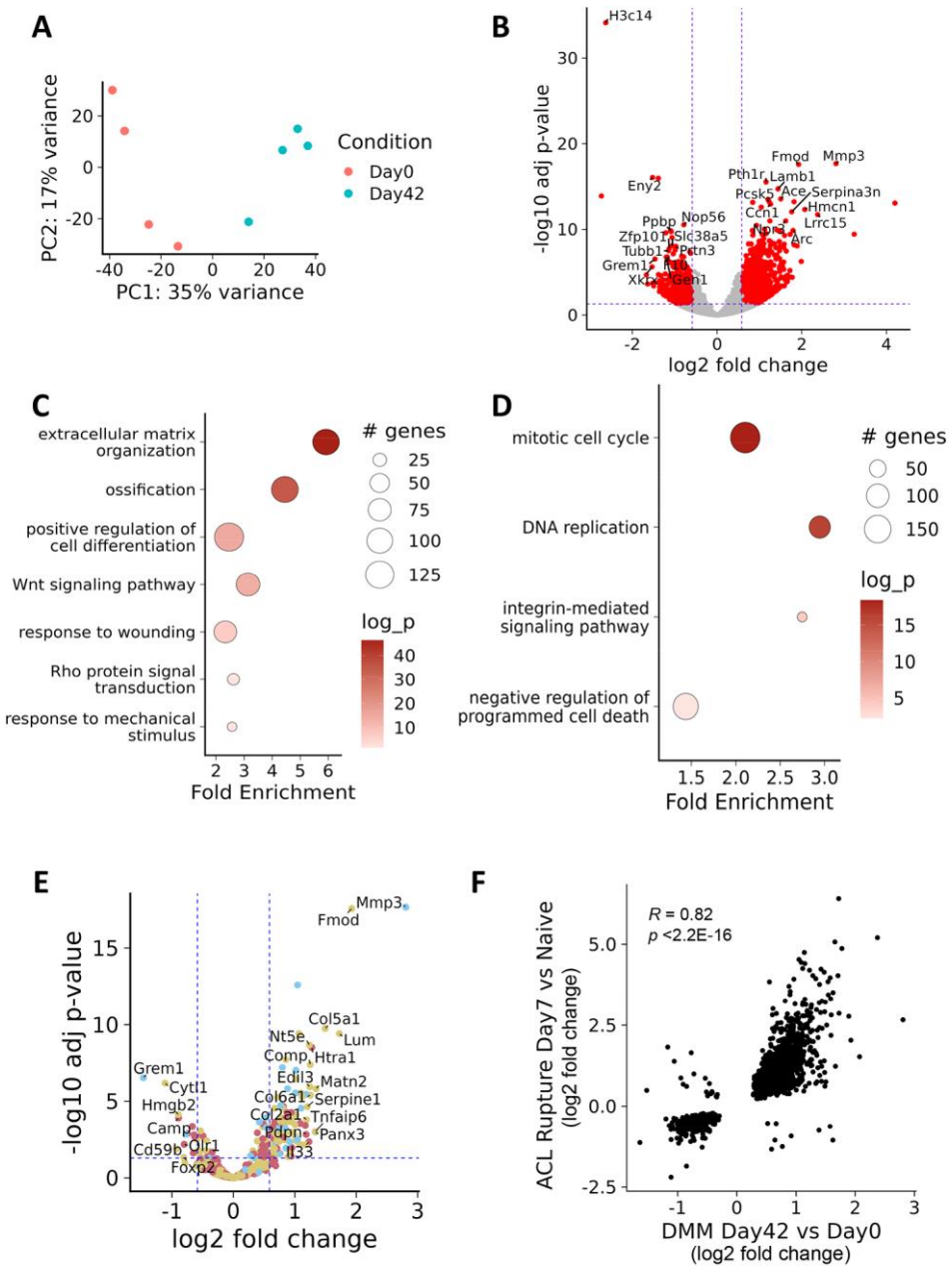

Fig. 2. Protective gene expression during DMM induction.

RNA-seq data from the DMM model of post-traumatic osteoarthritis comparing gene expression of RNA isolated from medial cartilage of Day 0 (pre-surgery - Naïve control animals versus animals 42 days post-surgery. (**A**) PCA plot of animals (n=4 per condition). (**B**) Volcano plot showing differential expression of all genes, red points indicate those significantly differentially expressed. Vertical blue lines indicate 1.5-fold change, horizontal - adjusted p-value <0.05. Pathway enrichment plots of the enriched gene ontology terms for the significantly up (**C**) and down-regulated (**D**) genes following DMM OA-induction. Selected gene ontology terms depicted. Circle

size represents the number of genes, the colour intensity depicts the fold enrichment -$\log_{10}$ p value (log_p). (**E**) Volcano plot of known OA affecting genes from Day 42 DMM vs control (Day 0). Genes which have detrimental, protective and ambiguous effects on OA are shown in yellow, red, and blue, respectively. Vertical blue lines indicate 1.5-fold change, horizontal - adjusted p-value <0.05. (**F**) Spearman correlation analysis of $\log_2$ fold expression of the significantly differentially expressed genes (FDR <0.05) from the ACL (Day 7 ACL vs Naïve control) and DMM (Day 0 vs Day 42) datasets.

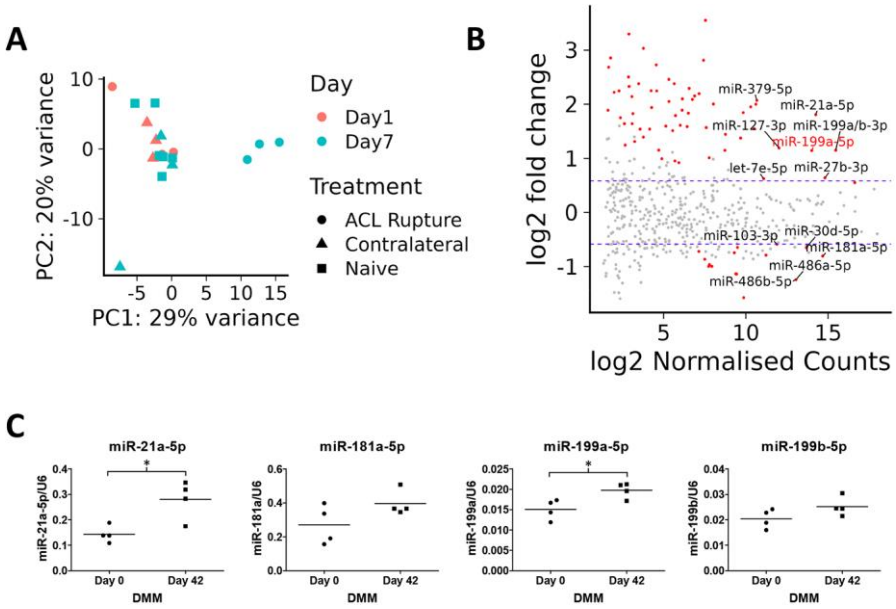

Fig. 3. miRNA differential expression upon abnormal mechanical loading.

(**A**) Principal component analysis plot showing of miRNA expression data from ACL model of post-traumatic osteoarthritis. (**B**) MA plot showing differential expression of most abundant miRNAs Day 7 ACL vs Naïve controls. Blue lines are 1.5 fold, red points are miRNAs significantly differentially expressed (FDR <0.05). miR-199a-5p is indicated in red. (**C**) Selected miRNA expression in RNA from micro-dissected cartilage prior to DMM (circles, Day 0) or 42 days post-surgery (squares, Day 42). Each data point represents a unique animal. Real-time PCR was performed in triplicate for each sample and normalised to the housekeeping *U6* small RNA using the calculation $2^{-(DCt)}$. Statistical comparisons were with an unpaired t test with Welch's correction, where * represents p <0.05.

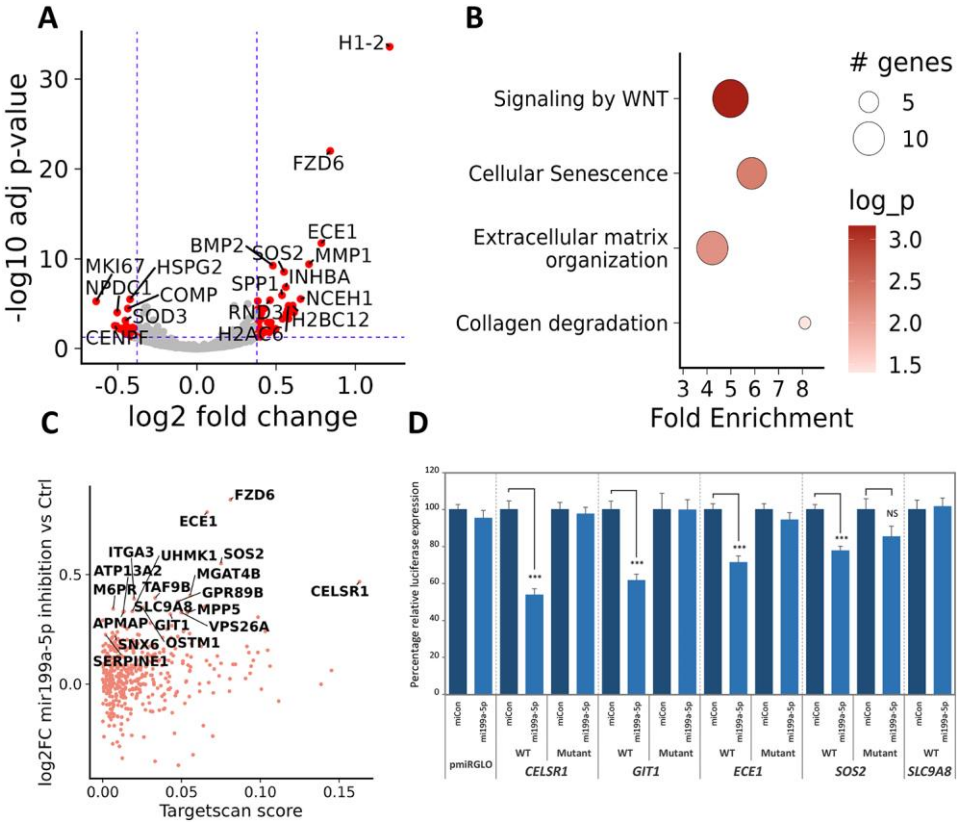

Fig. 4. Inhibition of miR-199a-5p induces a catabolic phenotype

(**A**) Volcano plot of differential expression of mir-199a-5p inhibition in human OA chondrocytes (n=4 donors). (**B**) Pathway enrichment plots of the enriched gene ontology terms for genes significantly differentially expressed following miR-199a-5p inhibition. Selected gene ontology terms depicted. Circle size represents the number of genes, the colour intensity depicts the fold enrichment -log10 p value (log_p). (**C**) Targetscan predicted scores of mir199a-5p targets and their differential expression after miR-199a-5p inhibition. (**D**) Testing miR-199a-5p predicted targets. The 3'UTRs of selected novel TargetScan predicted miR-199a-5p targets were cloned into the reporter vector pmiRGLO, transfected into SW1353 chondrosarcoma cells +/- miR-199a-5p mimic (light blue) or control non-targeting miR-mimic (miCon, dark blue). After 24 hours cells were lysed and Renilla and firefly luciferase levels determined, the former being using as an expression normaliser. Data were from four independent experiments performed in sextuplet and are expressed relative (percentage) to the respective 3'UTR reporter transfected along with miCon. Statistical comparisons were with an unpaired Student's *t*-test, where *** p<0.001. NS, not significant.

Table 1. Top similar transcriptomic responses identified in SkeletalVis

Accession	Comparison Description	Time point	Summary	Species	Cosine similarity zscore
GSE112641	Injured STR/ort vs Uninjured STR/ort	1 week post injury	Mechanical: ACL rupture	Mus musculus	5.62
GSE112641	Injured STR/ort vs Uninjured STR/ort	2 weeks post injury	Mechanical: ACL rupture	Mus musculus	5.34
GSE112641	Injured C57BL6 vs Uninjured C57BL6	2 weeks post injury	Mechanical: ACL rupture	Mus musculus	4.51
GSE121033	Surgery vs Non surgery	N/A	Surgical: ACLT	Mus musculus	4.42
E-MTAB-2923	Osteoblasts vs immature osteoblasts	4–6-week-old	Ex vivo: cell comparison	Mus musculus	4.03
GSE121033	Surgery with PC2 overexpression vs Non surgery	Unknown	Surgical: ACLT Lentiviral PC2 expression	Mus musculus	4.02
GSE41342	DMM surgery vs Sham	2 weeks post injury	Surgical: DMM	Mus musculus	3.63
GSE41342	DMM surgery vs Sham	16 weeks post injury	Surgical: DMM	Mus musculus	3.27
GSE112641	Injured MRL/MpJ vs Uninjured MRL/MpJ	2 weeks post injury	Mechanical: ACL rupture	Mus musculus	3.26
GSE33656	Frzb$^{-/-}$ vs wild-type	6-week-old	Genetic perturbation	Mus musculus	3.22

N/A not applicable or available. C57BL6, STR/ort, MRL/MpJ refer to mouse strains.

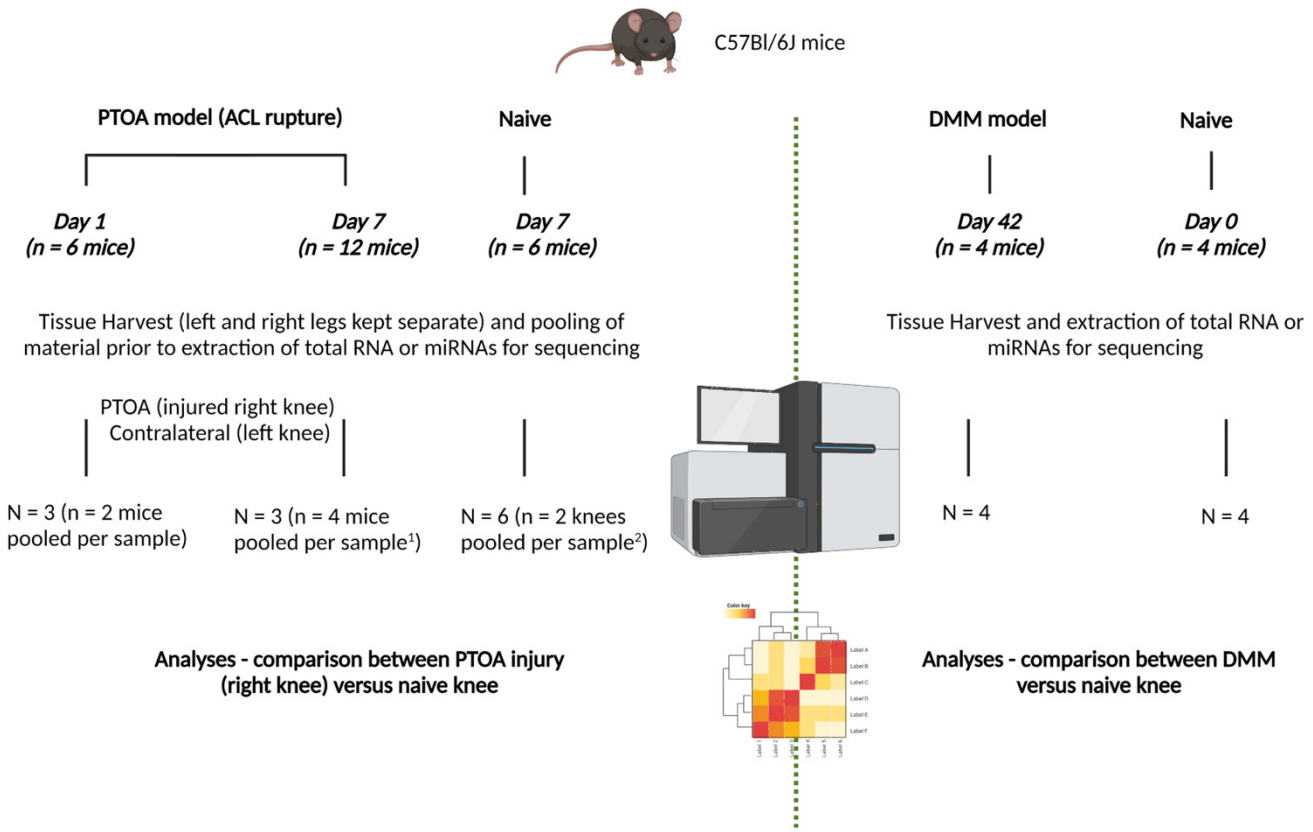

[1] 4 mice were pooled due to partial loss of cartilage at day 7
[2] Left and right knees were pooled separately for consistency with remainder of experiment

Fig. S1. Schematic of the experimental design and samples/animals used for RNA-seq

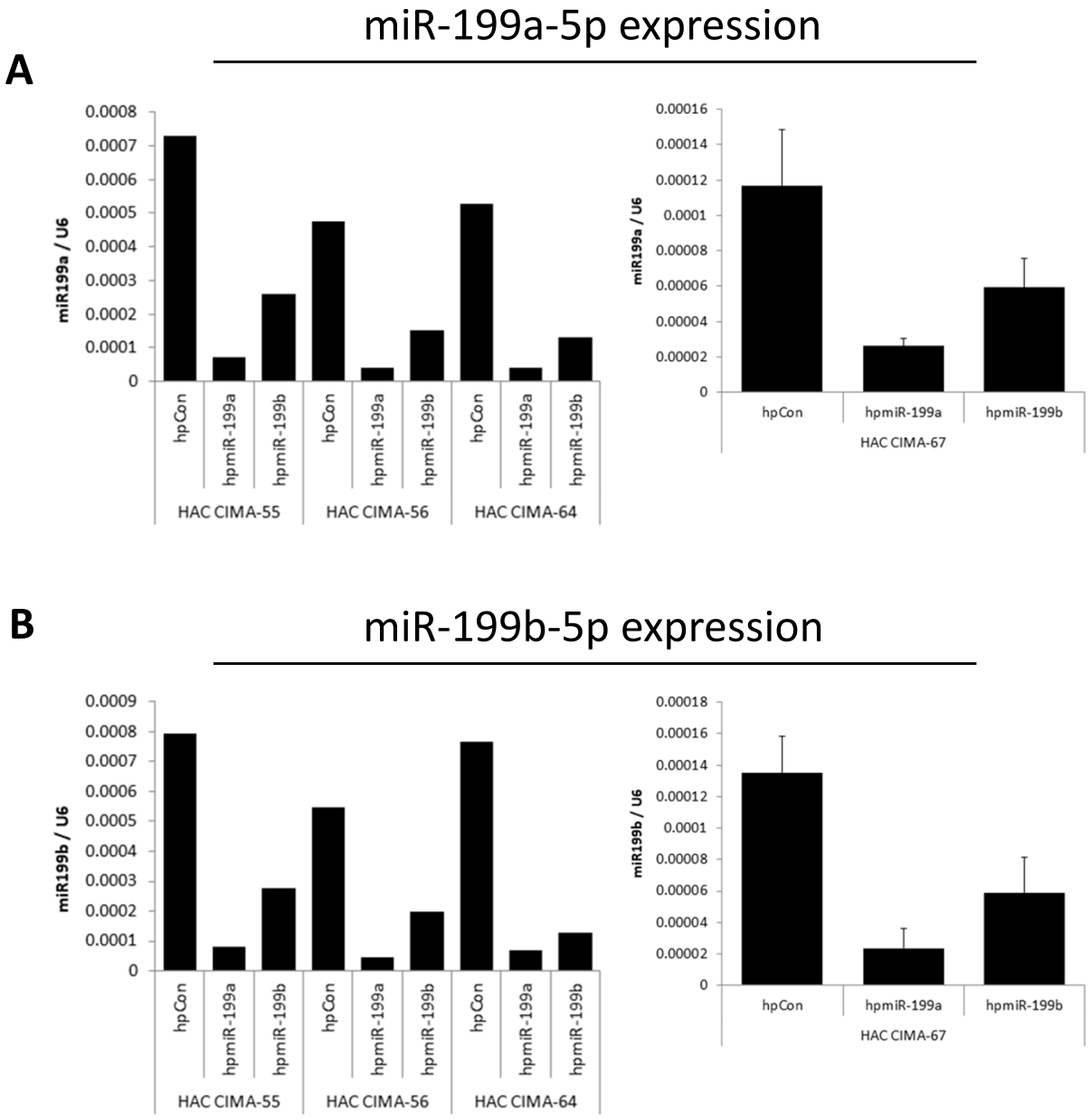

Fig. S2. Confirmation of inhibition of miR-199a-5p or miR-199b-5p in primary human articular chondrocytes used for RNA-seq

qRT-PCR measurement of miR-199a-5p (A) and miR-199b-3p (B) in four primary human articular chondrocyte donors (HAC), CIMA-55, -56, -64 and -67, following inhibition of the miRNA with the indicated control or targeting hairpin inhibitor. Note, the experiment for donor CIMA-67 was performed in triplicate. All data were normalised to the housekeeping short RNA U6. The hairpin inhibitors successfully inhibited the target miRNA but we were unable confirm isoform specificity. This could be because the either the inhibitors of the RT-qPCR assays cannot distinguish between miR-199a or b-5p. CIMA refers to the anonymous patient study ID.

Table S1.

Available for download at
https://journals.biologists.com/dmm/article-lookup/doi/10.1242/dmm.050583#supplementary-data

Table S2.

Available for download at
https://journals.biologists.com/dmm/article-lookup/doi/10.1242/dmm.050583#supplementary-data

Table S3.

Available for download at
https://journals.biologists.com/dmm/article-lookup/doi/10.1242/dmm.050583#supplementary-data

Table S4.

Available for download at
https://journals.biologists.com/dmm/article-lookup/doi/10.1242/dmm.050583#supplementary-data

Table S5.

Available for download at
https://journals.biologists.com/dmm/article-lookup/doi/10.1242/dmm.050583#supplementary-data

Table S6.

Available for download at
https://journals.biologists.com/dmm/article-lookup/doi/10.1242/dmm.050583#supplementary-data

Table S7.

Available for download at
https://journals.biologists.com/dmm/article-lookup/doi/10.1242/dmm.050583#supplementary-data

Table S8.

Available for download at
https://journals.biologists.com/dmm/article-lookup/doi/10.1242/dmm.050583#supplementary-data

Table S9.

Available for download at
https://journals.biologists.com/dmm/article-lookup/doi/10.1242/dmm.050583#supplementary-data

Table S10.

Available for download at
https://journals.biologists.com/dmm/article-lookup/doi/10.1242/dmm.050583#supplementary-data

Table S11.

Available for download at
https://journals.biologists.com/dmm/article-lookup/doi/10.1242/dmm.050583#supplementary-data